

Chaotic Response of a Limit Cycle

Kazuhisa Tomita¹ and Tohru Kai²

Received September 1, 1978

External periodic modulation of a nonlinear oscillator may lead to chaotic behavior. This phenomenon is attributed to the existence of a strange attractor, which embodies essentially a folding motion as is met within the Bernoulli shift or the baker's transformation. The results obtained for the Brussels model are discussed from this viewpoint.

KEY WORDS : Chaotic response ; turbulence ; stochastic description.

1. INTRODUCTION

In thermodynamic equilibrium it is known that the symmetry of a system may be lowered in a cooperative way when the system is energetically open to and is controlled by a heat reservoir. The ordered state which emerges as a result of such a transition is generally restricted to a regular spatial structure or pattern. In other words, equilibrium ordered states, although different from those of higher symmetry, are restricted to the fixed points of the motion. This is due to the time-reversal symmetry which is characteristic of thermodynamic equilibrium. In the neighborhood of equilibrium, time-reversal symmetry also leads to the Onsager reciprocity of transport coefficients.⁽¹⁾

When the system is controlled by more than one independent external reservoir the state of the system generally deviates from thermodynamic equilibrium. When the deviation is made large enough by external control there may appear new kinds of ordered states,^(2,3) namely, in addition to the fixed points which are familiar in thermodynamic equilibrium, there may appear recurring orbital motions which are structurally stable, thus forming new phases. In particular there appear periodic orbits which are known as limit cycles and are structurally stable. A limit cycle is a stable nonlinear

¹ Department of Physics, University of Kyoto, Kyoto, Japan.

² Department of Physics, Osaka City University, Osaka, Japan.

oscillation which exhibits much less amplitude response than a linear oscillator. The various kinds of characteristic biorhythms in living systems seem, from this point of view, not unrelated to their dynamic stability with respect to external perturbations.

Recently, however, a third phase, different from periodic orbits or fixed points, has come under serious consideration. This is connected with the appearance of a recurrent aperiodic orbit.^(4,5) Although the existence of such solutions has been known for some time, the recognition of the structural stability leading to a new "phase" belongs to relatively recent years, and the turbulence phenomenon in hydrodynamics has been reinterpreted from this point of view.⁽⁵⁾ The third variety may thus be called a "turbulent phase" in a wider context, as contrasted with "spatial pattern" or "temporal rhythm."

In this paper we discuss the third type of phase, namely the aperiodic or chaotic behavior of deterministic orbits, by way of an example which was treated in our previous papers.^(6,7) This is the case of forced oscillation of a nonlinear oscillator with two degrees of freedom. We thus discuss a chaotic response under a regular excitation.⁽⁸⁾

In Section 2 the results of a numerical computation are summarized in the form of a phase diagram and the motion in the phase plane is described in some detail using the stroboscopic representation. In Section 3 a one-dimensional discrete representation is invoked, and it is demonstrated that salient features of the behavior of the solution may be understood on the basis of known mathematical theorems^(12,17-20) for the one-dimensional case. Invariant measure, Liapunov number, and measure-theoretic entropy are estimated with respect to the asymptotic invariant manifold. The paper closes with a short discussion on the possible relevance of the chaotic response in a number of situations.

2. CHAOTIC RESPONSE OF A REACTING SYSTEM

The model we adopted is the one due to Prigogine, Lefever, and Nicolis (Brusselator)^(9,2,6,7) having two degrees of freedom under an external periodic excitation. It is shown in Fig. 1 schematically and is represented by the following set of equations:

$$dX/dt = X^2 Y - BX - X + A + a \cos \omega t \quad (2.1)$$

$$dY/dt = -X^2 Y + BX \quad (2.2)$$

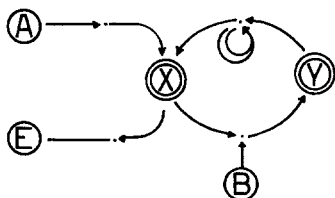
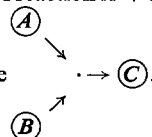


Fig. 1. The Brussels model. A reaction $A + B \rightarrow C$

is described by a scheme



where X and Y stand for the concentrations of the reference reactants, and A and B stand for those of the major reactants, which are assumed to be controllable. The last term on the right-hand side of (2.1) stands for the external periodic excitation having amplitude a and frequency ω .

According to the difference in character of the response or output behavior, a phase diagram can be obtained in the $a-\omega$ space, which is shown in Figs. 2a-2c.

As was described in our previous paper,^(7,8) a concise way of recognizing the output character is the stroboscopic representation,⁽¹⁰⁾ in which the successive points specifying the state of the system are plotted in the $X-Y$

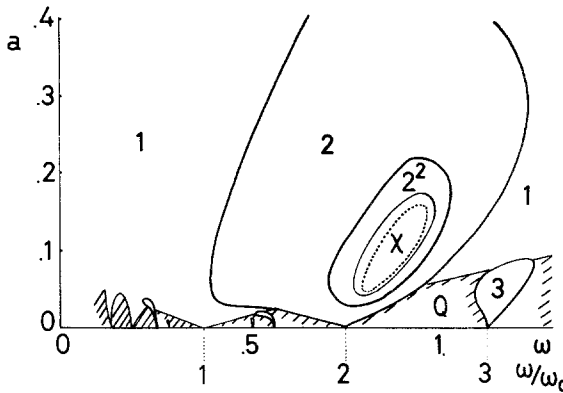


Fig. 2a. Phase diagram. The numbers indicate the periods of harmonic periodicity appearing in the respective regions. A stroboscopic limit cycle of nonintegral period appears in the shaded region Q , and a chaotic response is found in the region χ .

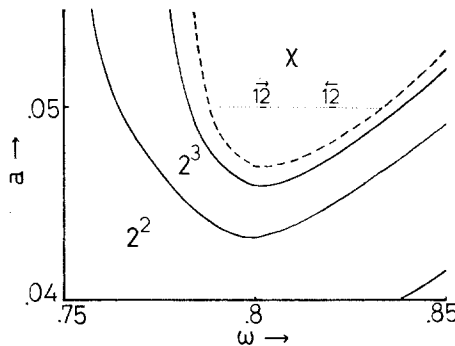


Fig. 2b. Enlarged view of the lowest part of χ and the neighborhood in Fig. 2a. The part of the line $a = 0.05$ inside the region χ is investigated in detail, and the results are summarized in Fig. 2c.

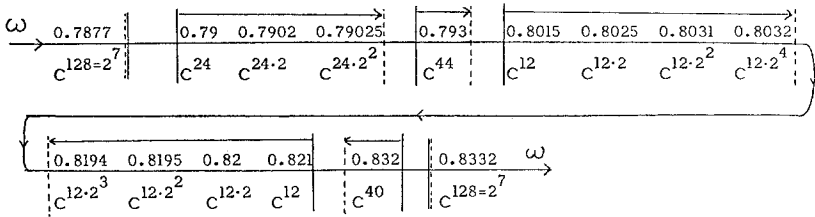


Fig. 2c. Schematic representation of the response in the region χ ($a = 0.05$). The arrows attached to the main horizontal line indicate the direction of increase in the applied frequency ω . The boundaries of the region χ are indicated by $||$ and $||$. Vertical solid lines across the main horizontal line designate points at which the basic period appears; the vertical broken lines designate points at which the cascade of bifurcations terminates. An arrow between two vertical lines indicates the direction of the successive bifurcations. C^n indicates a stable cycle of period n . The scheme corresponds to the window structure shown in Fig. 5. The regions in which successive bifurcations $C^{12} \rightarrow C^{12.2} \rightarrow C^{12.2^2} \rightarrow \dots$ appear are indicated by an additional solid line along the line $a = 0.05$ in Fig. 2b.

plane (phase plane) at instants separated by a regular time interval $\tau = 2\pi/\omega$. It is clear that a fixed point in this representation corresponds to a perfect entrainment, which appears in the region indicated by 1 (single-point periodicity). The region indicated by an integer n corresponds to n -point periodicity, and the region indicated by Q corresponds to a quasiperiodicity of the output, of which the stroboscopic phase portraits are a set of n fixed points and a closed orbit, respectively.

The subject to be discussed in this paper is, however, the behavior of the output in the region indicated by χ (chaotic or aperiodic).⁽⁸⁾ The stroboscopic phase portrait in this region is neither a fixed point nor a periodic orbit. Although the collection of asymptotic phase points forms an invariant manifold having a definite shape, the order in which the successive phase points appears in this manifold is chaotic and never looks periodic in a practical sense.

A typical example of the output behavior in this region is described in Fig. 3c, which corresponds to the set of parameter values $a = 0.05$ and $\omega = 0.81$. The four islands indicated by thick curves are the asymptotic invariant manifold formed by the stroboscopic portraits and the thin curves connecting these islands indicate the behavior of the system between the stroboscopic illuminations. The fact that the stroboscopic phase portrait consists of four separate islands implies that there exists an approximate four-point periodicity. That they are islands, however, indicates that deviations exist from the four-point periodicity, though they are not very large. Let us follow the order of numbers along the thinner curve and trace the behavior of the solution in more detail, starting from island ①. In the stage from ① to ②, the island ① is rotated by an angle π with little deformation. In the second

stage from ② to ③, the invariant manifold is folded roughly in the middle. In the third stage from ③ to ④, the whole island is rotated by an angle π with increasing folding. In the last stage of recursion from ④ to ①, the folded figure is pressed into an effective line element which coincides with the starting island ①. With repetition of this type of motion, i.e., similar to the baker's transformation, it is not difficult to realize that there results a complete mixing of all parts of the line element or island. Let us, for instance, imagine two orbits which are infinitesimally different at the outset. From the continuity of the mapping two representative points move close to each other in

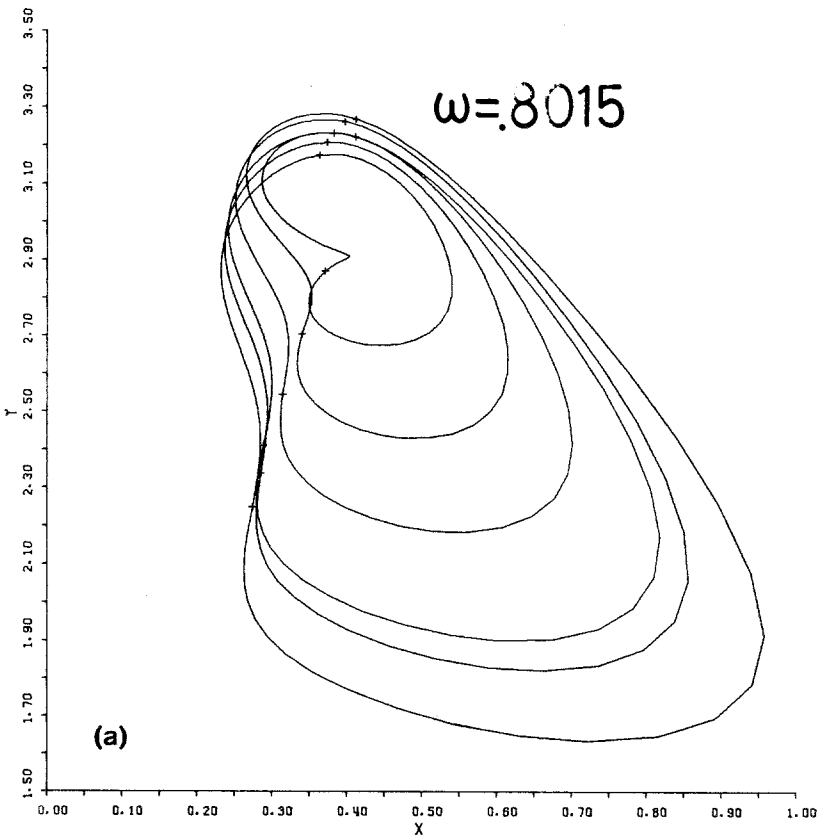


Fig. 3. Phase portrait in the region χ ($a = 0.05$). (a) $\omega = 0.8015$ corresponds to three-point periodicity (with respect to the mapping of an island onto itself). (b) $\omega = 0.81$ corresponds to a chaotic response. (c) $\omega = 0.81$: stroboscopic phase portrait. The four islands indicated by the thick curves correspond to the asymptotic invariant manifolds. The thin curves visiting these islands in the order of the attached numbers indicate the behavior of the system between the stroboscopic illuminations.

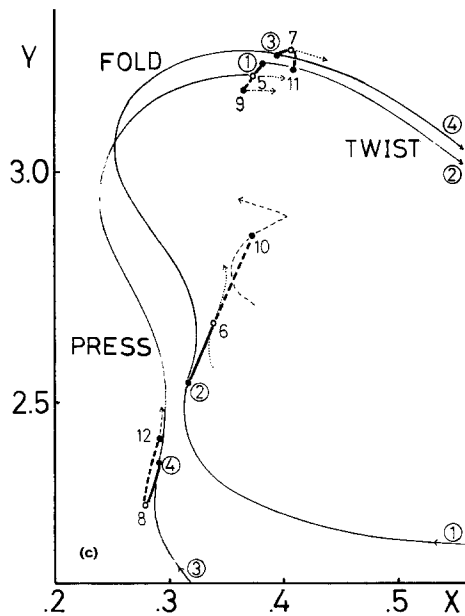
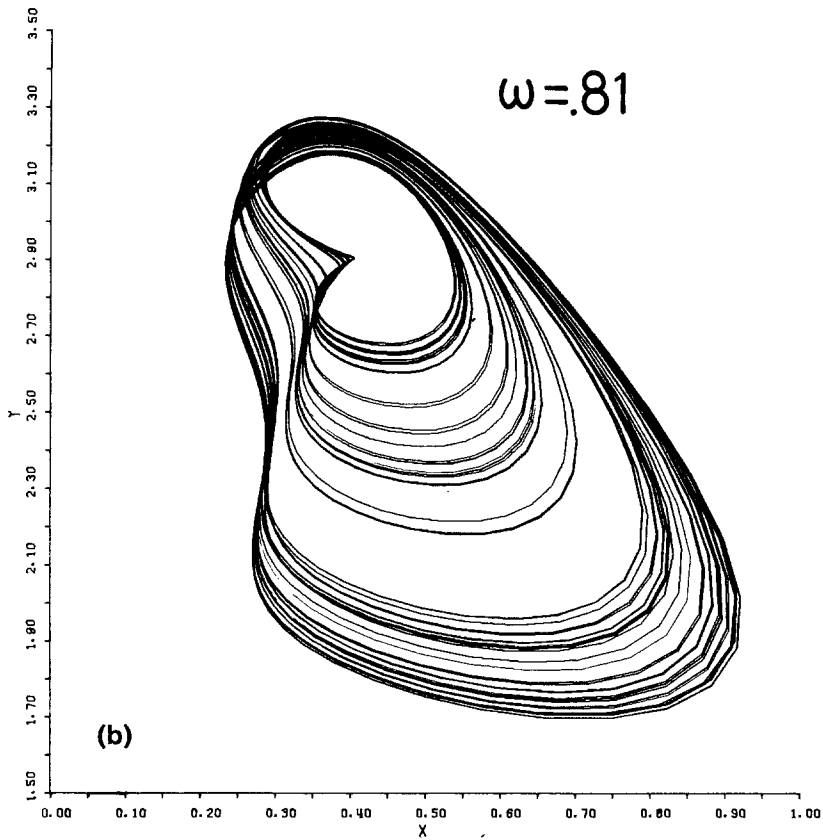


Fig. 3. Continued.

the early stage; however, eventually the distance between the two orbits can be arbitrarily large inside the island, and the correlation of the two motions definitely decreases. In other words, the motion of the phase point on the island exhibits no regularity and looks chaotic. The whole island, which is definitely an invariant of the motion, may be called a strange attractor,⁽⁵⁾ and it is a product of the infinite folding motion described above.⁽¹¹⁾ The decrease of the correlation is an essential fact in the observation of turbulence, and cannot be expected for a simple multiperiodicity. This led Ruelle to a new interpretation of hydrodynamic turbulence in terms of strange attractors.⁽⁵⁾

The shape of the asymptotic invariant manifold in our case looks practically one-dimensional, in spite of the two-dimensional frame of the phase portrait. This must be a reflection of the mechanism through which the strange attractor is built up. Let us start with an ensemble of the representative points which are all close to each other. Due to the orbital instability described above, the scale of the ensemble must be expanding at least in one direction. The existence of an asymptotic invariant manifold of a finite size, however, requires an essential recursion, which inhibits the infinite dilution of the original ensemble. A sufficient condition for the essential recursion is the existence of another direction along which the ensemble is contracting. When this is the case there appears a hyperbolicity in the phase plane which is transverse to the direction of flow.

When in addition the rate of contraction is sufficiently large as compared with that of expansion, which necessitates the folding, the final result of convolution is expected to be practically one-dimensional. In order to see the hyperbolicity of the orbital ensemble, it is clear that at least two degrees of freedom are needed. For a continuous flow, however, one can expect neither expansion nor contraction along the direction of the flow. Therefore, at least three degrees of freedom are needed in order to see the hyperbolicity in a continuous flow. Our example satisfies the minimum necessary condition in order to recognize the hyperbolicity, and it will be shown later that in fact such a hyperbolicity does exist in our case.

3. USE OF ONE-DIMENSIONAL ANALYSIS

As was seen in the previous section, the asymptotic manifold which is invariant under stroboscopic transformation looks almost one-dimensional in the present case. This suggests that in terms of a curvilinear coordinate the problem may be reduced to or at least simulated by a discrete mapping of a single variable, i.e.,

$$x_{i+1} = F(x_i) \quad (3.1)$$

where F is the *transfer function* characterizing the discrete mapping.⁽⁴⁾

One may resort then to the known properties and relations which have been proved mathematically for the one-dimensional problem.⁽¹²⁻¹⁵⁾ When Lorenz⁽⁴⁾ treated deterministic nonperiodic flow in the Bénard problem, he introduced a particular Poincaré map, i.e., the one-dimensional discrete representation of the continuous flow, and it was of significant help in anticipating the nonperiodic character of the solution. Let us introduce a one-dimensional map in the same spirit.

3.1. The Transfer Function

In introducing a one-dimensional representation into our problem it is convenient to consider island ② in particular, recognizing that the invariant manifold is almost linear in shape. One may then dispense with the introduction of a curvilinear coordinate, and just use the coordinate x (or y) in the one-dimensional parametrization. In Fig. 4 an example of the transfer function $F(x)$ obtained in this way is given. This particular example corresponds to the case of chaotic output inside the region χ . Note that F corresponds to a fourfold transformation in the stroboscopic scheme, because only island ② was chosen out of the four. In the numerical construction of the transfer function we notice several significant characteristics.

(i) The shape of the transfer function $F(x)$ is surprisingly simple and is almost quadratic in x . It is far from trivial that the motion obeys such a deterministic rule in spite of the seemingly chaotic character of the output.

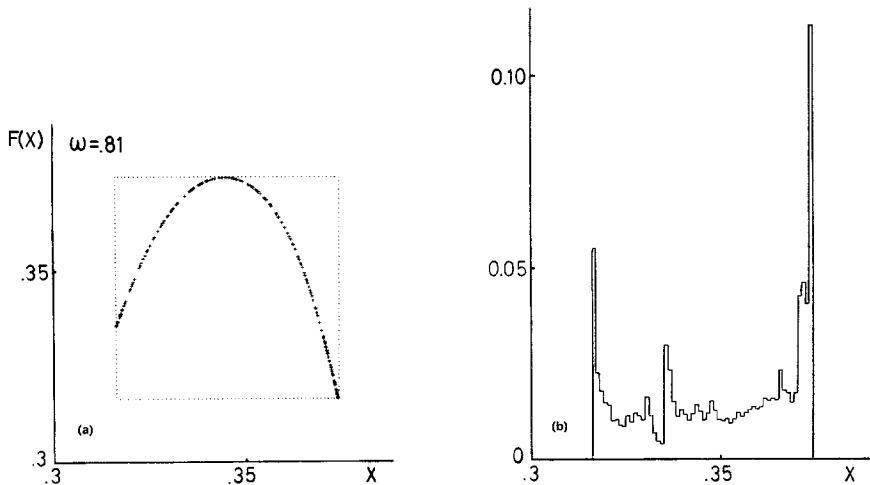


Fig. 4. (a) The transfer function $F(x)$ which governs the mapping of island ② onto itself ($a = 0.05$, $\omega = 0.81$). (b) Invariant measure based on histogram construction ($a = 0.05$, $\omega = 0.81$).

(ii) The domain on which the transfer function operates has definite limits at both ends ($x_m < x < x_M$). This reflects the fact that a finite interval of x is mapped repeatedly onto itself, being expanded and folded each time.

(iii) The whole domain of the transfer function is filled up by the calculated images; thus an apparently continuous function $F(x)$ is obtained.

Remembering that only n fixed points (or its definite multiple) can be expected when there is an n -point periodicity, this apparent continuity implies that there actually exists a practical chaos in the output.

3.2. Degree of Expansion $\lambda(x)$ of the Mapping

Suppose a point $x + \delta x$ in the neighborhood of point x is transferred to a point $F(x) + \Delta x$ through the mapping F . One can define the characteristic multiplier⁽¹²⁾

$$\lambda(x) \equiv |\Delta x / \delta x| = |dF/dx| \tag{3.2}$$

as a quantity measuring the degree of expansion of the mapping F at x . The condition $\lambda(x) > 1$ corresponds to an expanding map, and $\lambda(x) < 1$ to a contracting map. When x is chosen as a fixed point of the mapping F , it follows immediately that the fixed point x is stable if $\lambda(x) < 1$ and it is unstable if $\lambda(x) > 1$. For the special case in which x is a periodic point, $\lambda(x)$ is known as the Floquet multiplier.

Let us now consider the degree of expansion $\lambda^{(k)}(x)$ of the k -fold mapping

$$F^{(k)}(x) \equiv \overbrace{F \cdot F \cdots F}^k(x) \tag{3.3}$$

Then there exists the following relation, known as the chain rule⁽¹⁶⁾:

$$\begin{aligned} \lambda^{(k)}(x) &\equiv \left| \frac{dF^{(k)}(x)}{dx} \right| = \left| \frac{d}{dx} F(F^{(k-1)}(x)) \right| \\ &= \prod_{i=1}^{k-1} \left| \left(\frac{dF}{dy} \right)_{y=F^{(i)}(x)} \right| \quad \text{(chain rule)} \end{aligned} \tag{3.4}$$

Suppose in particular that x is chosen as one of the k -point periodic points $x_i^{(k)}$ ($i = 1, 2, \dots, k$); then each $x_i^{(k)}$ appears on the right-hand side of (3.4) just once, and thus the right-hand side does not depend on i . Consequently, the values of the derivative of the transfer function $F(x)$ at k periodic points $x_i^{(k)}$ are equal to each other. As a special case of this chain rule there exists the relation⁽¹⁴⁾

$$\lambda^{(2k)}(x_i^{(k)}) = \{\lambda^{(k)}(x_i^{(k)})\}^2 \tag{3.5}$$

Let us now examine the stability of k -periodic points as a function of an externally controlled parameter p . First the k -periodic points have to be

generated, and they must appear as a stable fixed point of a k -fold mapping in order to be observed at all. The conditions for such a situation may be written as follows:

$$F^{(k)}(x_i^{(k)}) = x_i^{(k)} \tag{3.6}$$

and

$$\left(\frac{dF^{(k)}}{dx}\right)_{x=x_i^{(k)}} \leq 1 \tag{3.7}$$

for a particular value p_1 of parameter p . The equality indicates the condition that the transfer function $F^{(k)}(x)$ initially becomes tangent to the straight line $y = x$, say on increasing p . This leads to the term *tangent bifurcation*.⁽¹⁵⁾

On increasing the parameter further one arrives at a second bifurcation at $p = p_2$, for which the condition

$$\left(\frac{dF^{(k)}}{dx}\right)_{x=x_i^{(k)}} = -1 \tag{3.8}$$

is satisfied. For this condition, however, the relation (3.5) ensures that

$$\left(\frac{dF^{(2k)}}{dx}\right)_{x=x_i^{(k)}} = 1 \tag{3.9}$$

This means that for $p > p_c$ the k periodic points $x_i^{(k)}$ ($i = 1, 2, \dots, k$) become unstable, but at the same time $2k$ periodic points are generated nearby through a tangent bifurcation. The whole process of destabilization and the generation of twice as many as stable fixed points is called a *harmonic* or *pitchfork bifurcation*.⁽¹⁵⁾ It is clear that on further increase in p there may appear a pitchfork bifurcation of the $2k$ periodic points into $4k$ -point

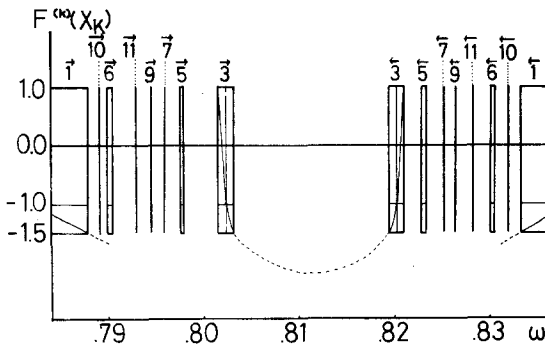


Fig. 5. Window structure (cf. Fig. 2c. The characteristic multiplier, or the degree of expansion, is plotted against the input frequency (a controlled parameter). The window specified by k corresponds to a region of stability for a series of harmonic bifurcations based on k -point periodicity (with respect to a mapping of an island onto itself). The arrow points toward the conjugate windows having the same basic periodicity. (k -point periodicity appears in a parenthesis pair.)

periodicity, and so forth. In this way a cascade of harmonic bifurcations indicated by $(2^n \times k)$ -point periodicity may appear on increasing p . It should be noted, however, that the intervals of p assigned to the consecutive stable periodicities become smaller as n increases, and the total sum of the series of intervals converges in such a way that an approximate relation

$$\lambda^{(2k)} \approx 3 - 2\{\lambda^{(k)}\}^2 \tag{3.10}$$

is valid for most of the harmonic bifurcations.⁽¹⁴⁾ This is obviously consistent with (3.8) and (3.9). It should further be noted that there exists a set of solutions

$$\lambda^{(2^n \times k)} \approx -1.5 \quad (\text{for all } k) \tag{3.11}$$

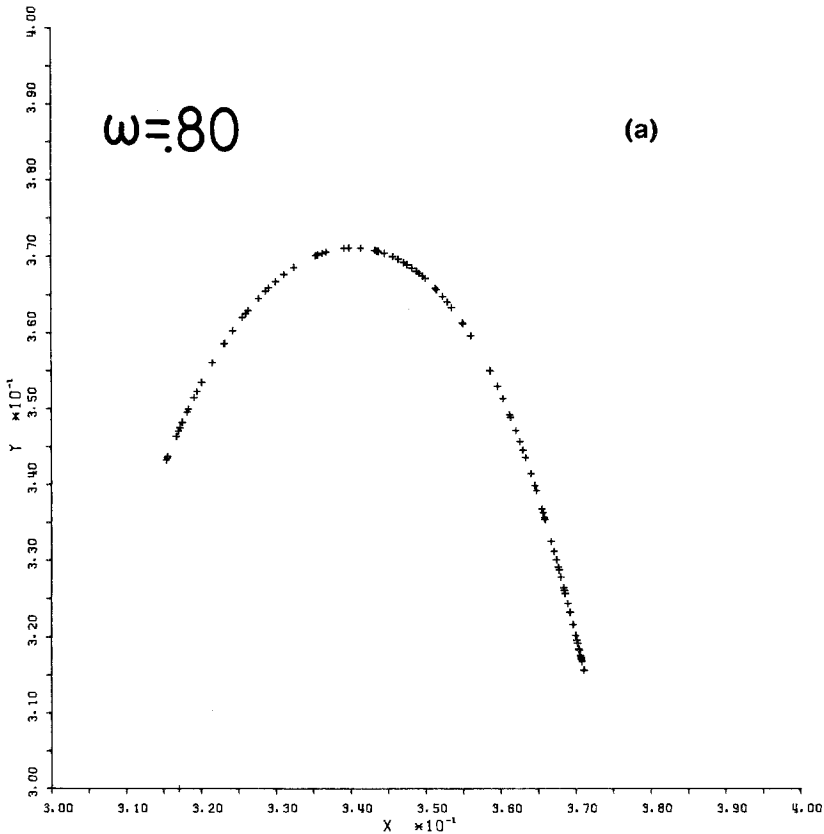


Fig. 6. Series of transfer functions suggesting window structure: (a) $\omega = 0.80$: To the left of the left window (left wall), chaotic. (b) $\omega = 0.8015$: Inside the left window of three-point periodicity. (c) $\omega = 0.81$: Between the two windows (middle wall), chaotic. (d) $\omega = 0.821$: Inside the right window of three-point periodicity. (e) $\omega = 0.825$: To the right of the right window (right wall), chaotic.

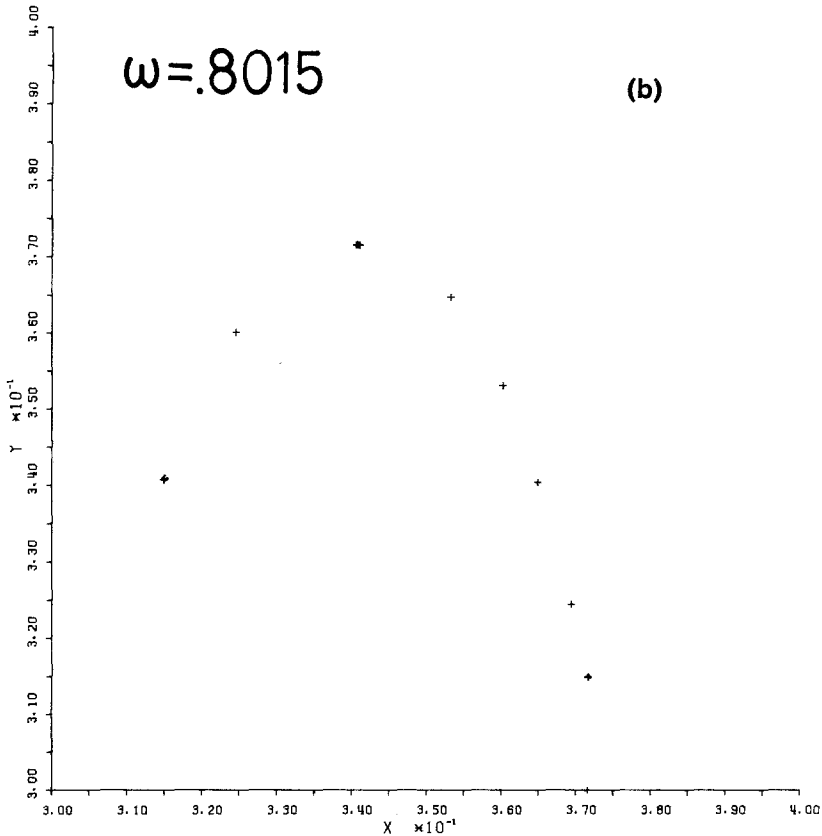


Fig. 6. Continued.

for a particular value p_∞ of the parameter p . The last relation (3.11) is connected with the fact that the whole family of $(2^n \times k)$ -point periodic points based on the k -point periodicity becomes unstable at $p = p_\infty$. The interval $p_1 \geq p \geq p_\infty$ which corresponds to the region of stability, belonging to the k -point periodicity [$1 \geq \lambda^{(k)}(x_i^{(k)}) \geq -1.5$] was called by May a "window".⁽¹⁵⁾

All the expectations stated above can be confirmed with our particular model, and the results are summarized in Fig. 5.

The input frequency ω was adopted as a controllable parameter and the window structure obtained by numerical analysis is indicated with reference to the value of $\lambda^{(k)} \equiv (dF^{(k)}/dx)_{x=x_i^{(s)}}$. One may note that each window starts when $\lambda^{(k)} = 1$, and when $\lambda^{(k)} = -1$ there appears the first harmonic bifurcation, which then cascades into a *curtain* of bifurcations until $\lambda^{(k)} = -1.5$, where everything becomes unstable, and the window terminates.

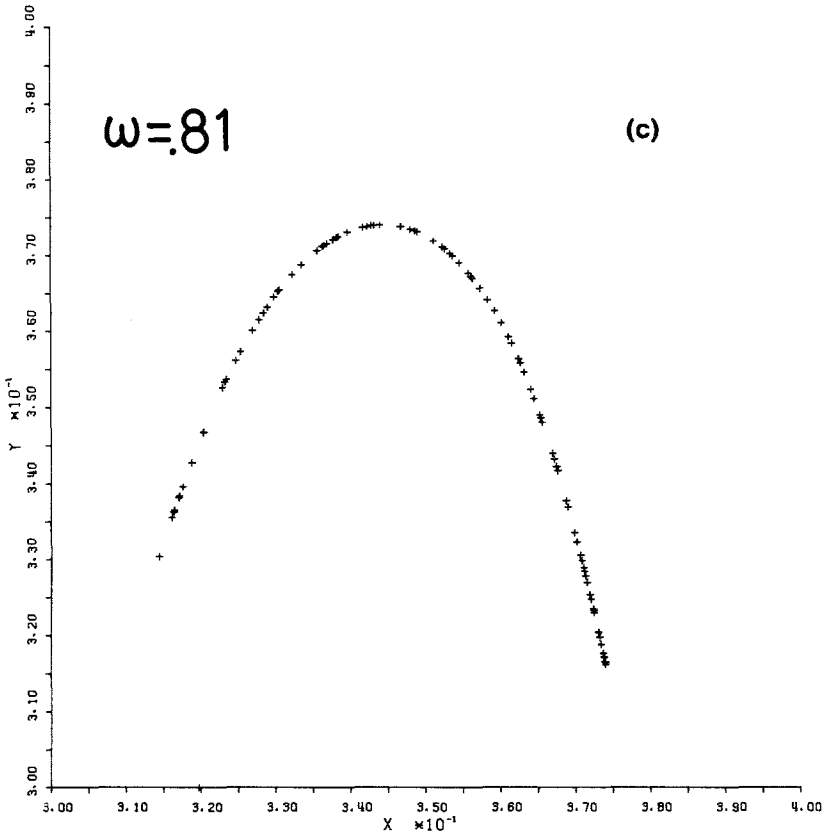


Fig. 6. Continued.

Between the windows specified by k -point periodicities there remain finite gaps which might be called a “wall.” It is in this wall region that one finds chaotic responses as described in the previous section. In Fig. 6 a series of transfer functions $F(x)$ is given for comparison. Comparing Fig. 6 with Fig. 5 according to the values of parameter ω , one may easily realize the existence of the window structure. It should also be recognized that the range of existence of k -point periodicity has both upper and lower limits in the parameter space for the present case. In other words, k -point periodic windows appear always as parenthetic pairs. Outside the parentheses no k -point periodicity exists, whereas between the two windows the whole harmonic family of k -point periodicity exists, but is unstable. Thus the wall region corresponds to chaotic output. It is also noted that odd k parentheses are embedded into other odd k parentheses according to increasing order of magnitude.

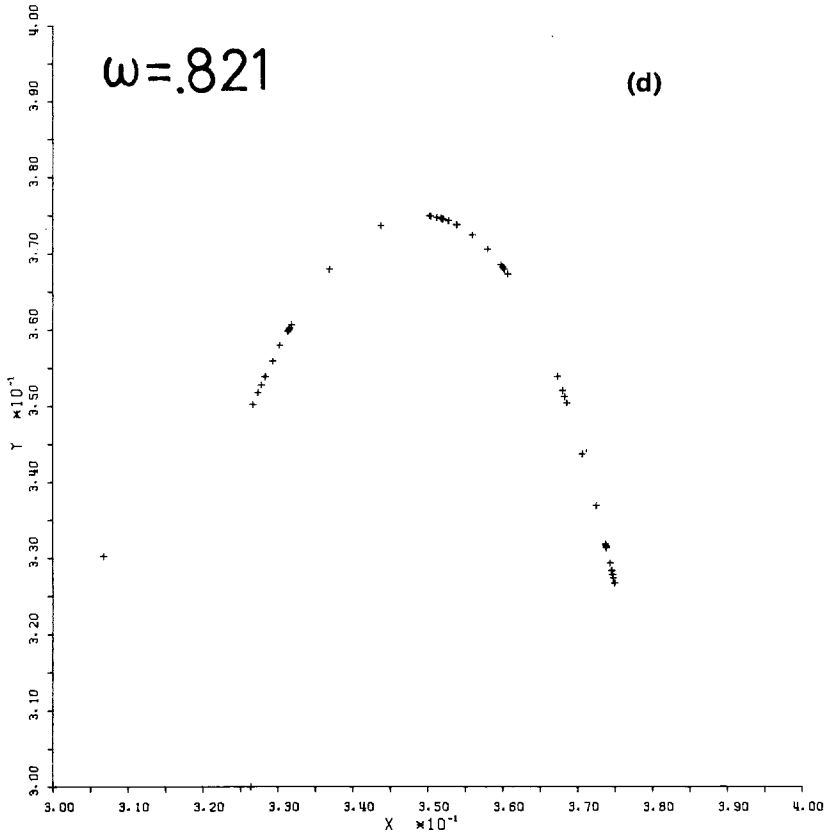


Fig. 6. Continued.

3.3. Theorem of Li and Yorke

Our natural concern lies in the content of the seemingly chaotic output, for on the practical level one is usually unable to distinguish an aperiodic motion from a periodic motion of long period. In this connection Li and Yorke⁽¹²⁾ have shown that mathematically both types of motions are bound to *coexist*. Motivated by the earlier work of Lorenz,⁽⁴⁾ Li and Yorke proved a remarkable mathematical theorem for the solution of the one-dimensional difference equation (3.1), and a number of applications have also been discussed.⁽¹⁶⁻¹⁹⁾ It is remarkable because it secures the possibility of chaotic behavior in a simple deterministic model, a problem which is related to the theory of ergodicity and of turbulence. According to their theorem the following statements are proved:

Suppose there exists a genuine three-point cycle with respect to the

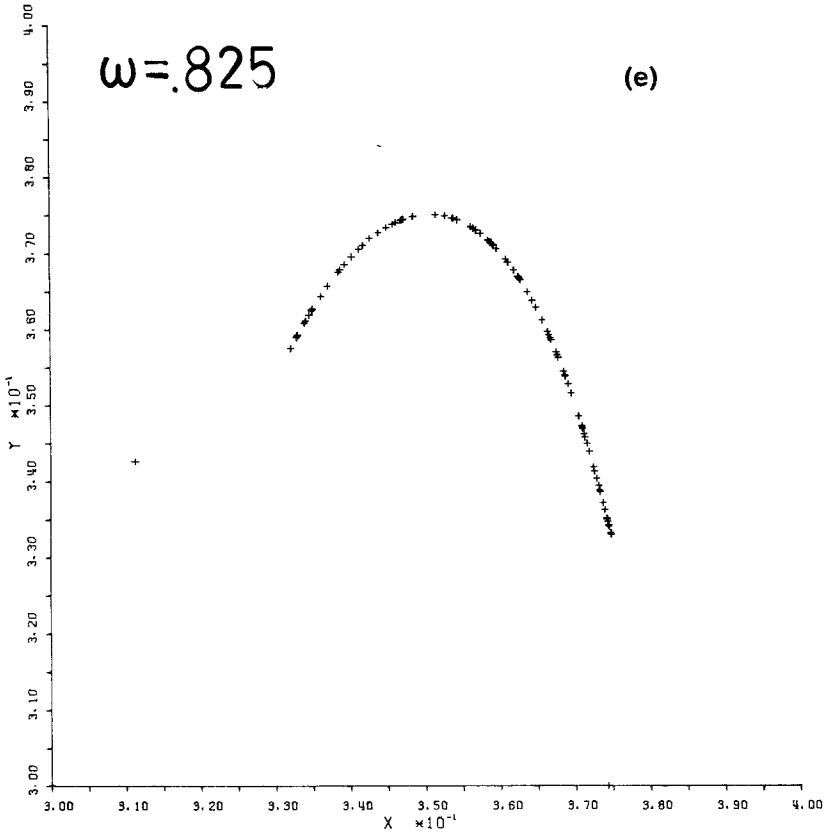


Fig. 6. Continued.

mapping F given in (3.1), i.e., a solution such that $x_{n+3} = x_n$ with $x_{n+2} \neq x_n$ and $x_{n+1} \neq x_n$.

(I) It then necessarily follows that there are also cycles with period k , where k is any positive integer.

(II) Furthermore, there exists an uncountable number of initial points x_0 from which the system does not eventually settle into any of these cycles (i.e., not “asymptotically periodic,” or simply “aperiodic”).

The three-point cycle in the premise has since been generalized to five-, seven-,⁽¹⁸⁾ and then to $[k (\neq 2^n)]$ -point cycles.⁽¹⁹⁾ Concerning the statement (I), it was independently shown by Sarkovskii⁽²⁰⁾ and Stefan⁽¹⁷⁾ that there exists the following directed series:

$$\begin{aligned}
 3 \vdash 5 \vdash 7 \vdash \dots \vdash 2 \cdot 3 \vdash 2 \cdot 5 \vdash 2 \cdot 7 \vdash \dots \vdash 2^2 \cdot 3 \vdash 2^2 \cdot 5 \vdash 2^2 \cdot 7 \vdash \dots \\
 \vdash 2^3 \vdash 2^2 \vdash 2 \vdash 1
 \end{aligned}
 \tag{3.12}$$

Namely, where the existence of a k -point cycle is presupposed, the existence of all the periodicities standing to the right of k necessarily follows. One may easily recognize that this order is followed in the window structure of the present model.

As has been pointed out in the process of proving (3.12), the condition for an (odd- k)-point cycle to be a possible cycle of the lowest order is that the consecutive image points should be traced in the order (or its entire reverse) indicated in Fig. 7.

Why does the existence of such periodic orbits lead to aperiodic orbits? The basic fact here is the recurrent property of the asymptotic motion under the original mapping. Both periodic and aperiodic motions can be the manifestation of this property. From this point of view the existence of a periodic orbit implies the recurrent property of the mapping itself, and this in turn requires the possible aperiodic motion to be recurrent. For such aperiodic motions to be actually observed, it suffices that all the possible periodic motions are unstable. In this situation the orbit has to come back to the neighborhood of the original point after some excursion, as suggested by Fig. 7. A possibility then arises that the mapping of a small interval is not necessarily unique, and that various different periodicities may exist. However, the image point can never settle into the original point, because any periodic orbit is unstable, and is repeatedly diverted into a further excursion, which naturally leads to a recurrent aperiodic motion. The wall between the two windows of three-point cycles seems exactly the region in which the aperiodic motion is to be observed, for all the periodic motions are orbitally unstable, but other walls may be candidates as well.

3.4. Invariant Measure and Liapunov Number

In Fig. 4 a pseudocontinuous representation of the transfer function $F(x)$ was obtained in the interval $x_m < x < x_M$. One may then provide this

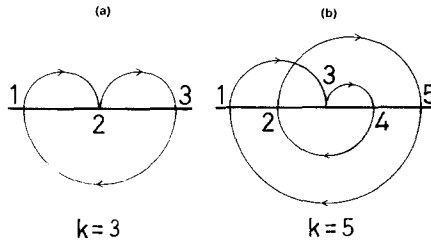


Fig. 7. Snapback property of the minimal cycle. (Schematic). The points belonging to an (odd- k)-point cycle should be mapped in the indicated order, in order for this particular cycle to be the minimal cycle. (a) $k = 3$, (b) $k = 5$.

invariant interval with a definite measure, simply by constructing the histogram, associating to each image point a common weight. For instance, the measure obtained by N image points, starting from the initial point x_0 , may be defined by⁽²¹⁾

$$\mu_{x_0, N}(x) = \frac{1}{N} \sum_{i=0}^{N-1} \delta(x - F^{(i)}(x_0)) \quad (3.13)$$

When N is taken large enough, it is expected that $\mu_{x_0, N}(x)$ becomes independent of (x_0, N) ; therefore the limit quantity may be interpreted as an invariant measure, i.e.,

$$\mu(x) = \lim_{N \rightarrow \infty} \mu_{x_0, N}(x) \quad (3.14)$$

where the ergodic property is tacitly assumed.

For our particular case the approximate measure constructed in this way is indicated in Fig. 4 for $N = 1000$.

There is another quantity which is closely related to the invariant measure. It is the *Liapunov number* $\chi(x_0)$.⁽²¹⁻²³⁾ This is a *characteristic exponent* associated with the rate of magnification of the neighborhood of a point x_0 , and is defined by

$$\begin{aligned} \chi(x_0) &\equiv \lim_{n \rightarrow \infty} \frac{1}{n} \log \left| \left(\frac{dF^{(n)}}{dx} \right)_{x=x_0} \right| \\ &= \lim_{n \rightarrow \infty} \frac{1}{n} \sum_{k=0}^{n-1} \log \left| \left(\frac{dF}{dx} \right)_{x=x_k} \right| \end{aligned} \quad (3.15)$$

where $x_k = F(x_{k-1})$ and the second expression follows from the chain rule (3.4). One may note from (3.2) that the Liapunov number $\chi(x_0)$ provides the rate of repulsion between nearby orbits. It naturally follows that $\chi(x_0) < 0$ for an attractor, $\chi(x_0) > 0$ for a repeller, and $\chi(x_0) = 0$ for marginal situations.

In the particular case in which motion along the invariant manifold is ergodic, the Liapunov number $\chi(x_0)$ is expected to be positive and independent of the initial point x_0 , $\chi(x_0) = \chi$ being a constant characterizing the invariant manifold as a whole.

In the present model $x_m \simeq 0.316$, $x_M \simeq 0.376$, and the Liapunov number is computed to be $\chi = 0.536$. The independence on the initial point suggests that a mixing actually occurs as a result of the aperiodic motion along the invariant manifold.

It is known that the Liapunov number χ is in some cases equivalent to the *topological entropy* ψ ,⁽²¹⁾ which is based on the number of periodic orbits and is defined by

$$\begin{aligned} \psi &\equiv \lim_{n \rightarrow \infty} (1/n) \\ &\times \log[\text{number of fixed points under the mapping } F^{(n)}] \end{aligned} \quad (3.16)$$

It is also related to the measure-theoretic entropy $h(\mu)$ through the measure μ assigned to the invariant manifold. Bowen and Ruelle⁽²⁴⁾ have shown that there exists a relation

$$h(\mu) - \int \mu(dx) \chi_+(x) \leq 0 \quad (3.17)$$

where $\chi_+(x)$ is $\chi(x)$ in the one-dimensional case. For the general multi-dimensional case χ_+ is defined by a sum of products of positive χ and the dimension of its eigenspace.

Suppose the situation is similar to the case of the axiom A system; μ may be determined from (3.17) as that which maximizes the lefthand side expression.

As $\chi_+(x)$ is independent of x in our particular case, it is concluded then that $h = \chi = 0.536$, provided the measure μ is normalized.

4. THE WIDTH OF THE QUASI-ONE-DIMENSIONAL INVARIANT MANIFOLD

In Section 3 the mathematical properties of truly one-dimensional mapping were found to be of significant help in describing the behavior of a two-dimensional diffeomorphism, of which the stroboscopic portrait of the invariant manifold looks almost one-dimensional. Naturally, however, the approximation to a two-dimensional diffeomorphism in terms of a one-dimensional noninvertible mapping has its own limitation. In this connection one has carefully to examine the fine-scale plot of part of the seemingly one-dimensional manifold in our computer simulation, as shown in Fig. 8. One

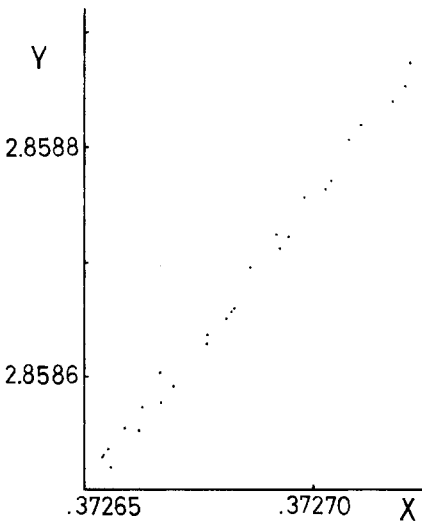


Fig. 8. Fine-scale plot of the quasi-one-dimensional invariant manifold indicating finite width, of the order of 10^{-5} . All the figures correspond to the uppermost part of the island ② ($a = 0.05$, $\omega = 0.81$).

may note then a finite width of the quasi-one-dimensional manifold, which is of the order of 10^{-5} . This is to be compared with the overall length of the manifold, which is of the order of 10^{-1} .

In what follows a method is given of estimating the width of the manifold in a perturbative way.^(25,26) The idea is to convert the one-dimensional non-invertible map $x_{n+1} = F(x_n)$, defined by (3.1) in Section 3, back into a two-dimensional homeomorphism, of which the one-dimensional map remains a good first approximation insofar as the invariant manifold is concerned.

This can be done by introducing a small second coordinate y as follows:

$$x_{n+1} = F(x_n) + y_n, \quad y_{n+1} = ax_n \quad (|a| \ll 1) \quad (4.1)$$

Here a indicates the relative scale of spread in y to that in x , and $a = 0$ corresponds to the one-dimensional map, which has nonunique inversion. With $a \neq 0$ the unique inversion is given by

$$x_n = y_{n+1}/a, \quad y_n = -F(y_{n+1}/a) + x_{n+1} \quad (4.2)$$

Let us now examine the modes of expansion of the neighborhood of a point (x, y) which belongs to the invariant manifold. For the mode characterized by a characteristic multiplier m , the small deviation $(\Delta x, \Delta y)$ from the point satisfies the linearized relation

$$m \begin{pmatrix} \Delta x \\ \Delta y \end{pmatrix} = \begin{pmatrix} \lambda & 1 \\ a & 0 \end{pmatrix} \begin{pmatrix} \Delta x \\ \Delta y \end{pmatrix} \quad (4.3)$$

where $\lambda \equiv F'(x)$. This leads to an equation for m :

$$m^2 - \lambda m - a = 0 \quad (4.4)$$

from which one finds

$$m = \frac{1}{2} \{ \lambda \pm (\lambda^2 + 4a)^{1/2} \} \quad (4.5)$$

As $|a| \ll 1$ the two modes are characterized by

$$m_1 \cong \lambda \quad \text{and} \quad m_2 = -a/\lambda \quad (4.6)$$

A computer estimation was made of the two characteristic multipliers on our original model. As an example the successive mappings in the neighborhood of a point of four cycles were computed, and m_1 and m_2 were found to be of the order of unity and 10^{-4} , respectively. This implies that $a \approx -10^{-4}$ at this point.

Supposing that a is common to the entire invariant manifold, which is reflected by the width approximately, Eq. (4.1) is now completely specified. One may then solve (4.1) in an iterative way, i.e., in the form of an expansion in terms of the small quantity a , and find the invariant manifold directly. From (4.1) one finds the relation

$$x_{n+1} = F(y_{n+1}/a) + y_n \quad (4.7)$$

In the spirit of Bridges and Rowlands,⁽²⁶⁾ the zeroth-order approximation to the invariant manifold is given by

$$x = F(y/a) \quad (4.8)$$

neglecting the second term on the right-hand side. In first order, the approximate invariant manifold is given by

$$x = F(y/a) + aF^{-1}(y/a) \quad (4.9)$$

The next order approximation is given by

$$x = \{F + a(F + aF^{-1})^{-1}\}(y/a) \quad (4.10)$$

and so forth.

For a single-humped function F the inverse F^{-1} is two-valued, and this type of inversion appears repeatedly in the above construction. This implies that the calculated invariant manifold consists of infinitely many branches or foldings. However, it is also clear from the above construction that the relative scale of the overall spread of the invariant manifold in y with respect to that in x is given by a .

The relative scale 10^{-4} found from the simulation in Fig. 8 is in fact of the same order as the $a \approx 10^{-4}$ determined independently from the anisotropy in characteristic multiplier. This justifies the above method of construction on the one hand, and on the other it demonstrates that the observed small spread of the invariant manifold is in fact nontrivial, i.e., noninstrumental, and has its origin in the nonlinear dynamic folding.

The idea of one-dimensional approximation lies in the neglect of the difference of the order of the width, i.e., the order of 10^{-5} , in the values of x . Let us suppose two points initially separated by this order of magnitude along the invariant manifold. On each step of the mapping this difference is magnified by a factor e^χ . How many steps, then, does it require for this difference to become comparable with the total span of x , which is of the order of 10^{-1} ? For the special case in which $a = 0.05$ and $\omega = 0.81$ this critical number of steps n satisfies the following relation:

$$e^{n\chi} \times 10^{-5} \approx 10^{-1} \quad (4.11)$$

By using the estimated value $\chi = 0.536$, n is estimated as

$$n \gtrsim 17 \quad (4.12)$$

This implies that after 17 steps of mapping, the one-dimensional approximation loses its strict validity. At the same time, however, the mixing is completed under the same condition.

5. SUMMARY AND DISCUSSION

Using a typical model (the Brussels model), the chaotic response of a limit cycle to an external periodic excitation has been investigated in detail with the stroboscopic representation. Chaotic outputs have been found for intermediate values of the input amplitude and frequency lying inside the region of subharmonic resonance. The asymptotic invariant manifold looks almost linear in the two-dimensional phase plane. Mathematical theorems established for a one-dimensional system were found to be of significant help in anticipating and describing the behavior of the chaotic output under consideration. In reality, however, it was also demonstrated that the quasi-linear invariant manifold has its own width, of the order of 10^{-4} , which is associated with the folding construction of the strange attractor.

Time-independent external control may also lead to chaotic output; however, the choice of Poincaré map is more difficult in this case.

It is not clear whether the cascade of harmonic bifurcations, though undoubtedly one of the typical situations pointing to chaos, is the unique symptom of chaos or not. The relation between the appearance of homoclinic orbits and the cascade of bifurcations should be the subject of future investigations.

One final comment on the definition of chaos: It is obvious that the finite accuracy of any physical measurement or computer simulation inhibits a clear-cut distinction among (a) long enough transient motions, (b) periodic motions with long enough period, and (c) aperiodic motions. For instance, even the sensitive dependence on initial condition may not distinguish the above three cases. In this situation physicists have to look for some appropriate quantity which may describe the practical chaos, while possibly covering mathematically different situations. In this connection the theorem of Li and Yorke may be taken to assert the coexistence of (b) and (c). Suppose in addition one may find a quantity which is practically common between the two cases; then it would be of great use in describing physical chaos. The connection between the Liapunov characteristic exponent [associated with (c)] and the fixed point distribution [associated with (b)] would be an extremely interesting subject of study from this point of view.

REFERENCES

1. L. Onsager, *Phys. Rev.* **37**:405 (1931); **38**:2265 (1931).
2. P. Grandsorff and I. Prigogine, *Thermodynamic Theory of Structure, Stability and Fluctuations* (Wiley, New York, 1971).
3. G. Nicolis and I. Prigogine, *Self-Organization in Nonequilibrium Systems* (Wiley, New York, 1977).
4. E. N. Lorenz, *J. Atmos. Sci.* **20**:130 (1963).

5. D. Ruelle and F. Takens, *Comm. Math. Phys.* **20**:167 (1971); **23**:343 (1971).
6. K. Tomita, T. Kai, and F. Hikami, *Prog. Theor. Phys.* **57**:1159 (1977).
7. T. Kai and K. Tomita, *Prog. Theor. Phys.* **61**:54 (1979).
8. K. Tomita and T. Kai, *Phys. Lett.* **66A**:91 (1978); K. Tomita and T. Kai, OJI Seminar, Kyoto (July 1978); *Prog. Theor. Phys.* **57**:280 (1978).
9. I. Prigogine and R. Lefever, *J. Chem. Phys.* **48**:1695 (1968); R. Lefever, *J. Chem. Phys.* **48**:4977 (1968); R. Lefever and G. Nicolis, *J. Theor. Biol.* **30**:267 (1971).
10. N. Minorsky, *Nonlinear Oscillations* (Van Nostrand, 1962).
11. S. Smale, *Bull. Am. Math. Soc.* **73**:747 (1967).
12. T. Y. Li and J. A. Yorke, *Am. Math. Mon.* **82**:985 (1975).
13. R. M. May, *J. Theor. Biol.* **52**:511 (1975).
14. R. M. May and G. F. Oster, *Am. Natur.* **110**:573 (1976).
15. R. M. May, *Nature* **261**:459 (1976).
16. P. A. Samuelson, *Foundations of Economic Analysis* (Harvard, 1947), p. 390.
17. P. Stefan, *Comm. Math. Phys.* **54**:237 (1977).
18. M. B. Nathanson, *J. Combinat. Theor. (A)* **22**:61 (1977).
19. Y. Oono, *Prog. Theor. Phys.*, to appear.
20. A. N. Sarkovskii, *Ukr. Mat. Zh.* **16**:61 (1964).
21. D. Ruelle, in *Proc. Int. Math. Phys. Conf.* (Rome, 1977), to appear.
22. G. Benettin, L. Galgani, and J. Strelcyn, *Phys. Rev. A* **14**:2338 (1976).
23. T. Nagashima and I. Shimada, *Prog. Theor. Phys.* **58**:1318 (1977); I. Shimada and T. Nagashima, *Prog. Theor. Phys.*, to appear.
24. R. Bowen and D. Ruelle, *Inventions. Math.* **29**:181 (1975).
25. M. Hénon, *Comm. Math. Phys.* **50**:69 (1976).
26. R. Bridges and G. Rowlands, *Phys. Lett.* **63A**:189 (1977).